Cell Research (2013) 23:290-299.

www.nature.com/cr

ORIGINAL ARTICLE

Cytokinin signaling regulates pavement cell morphogenesis in *Arabidopsis*

Hongjiang Li[1, 2, 3, 4], Tongda Xu[1, 5], Deshu Lin[1, 6], Mingzhang Wen[1], Mingtang Xie[1], Jérôme Duclercq[3, 4], Agnieszka Bielach[3, 4], Jungmook Kim[7], G Venugopala Reddy[1], Jianru Zuo[8], Eva Benková[3, 4], Jiří Friml[3, 4], Hongwei Guo[2], Zhenbiao Yang[1]

[1]Center for Plant Cell Biology, Department of Botany and Plant Sciences, University of California, Riverside, CA 92521, USA; [2]State Key Laboratory of Protein and Plant Gene Research, College of Life Sciences, Peking University, Beijing 100871, China; [3]Department of Plant Systems Biology, VIB, Technologiepark 927, B-9052 Gent, Belgium; [4]Department of Plant Biotechnology and Bioinformatics, Ghent University, Technologiepark 927, Gent B-9052, Belgium; [5]Temasek Life Sciences Laboratory, 1 Research Link, National University of Singapore, Singapore 117604, Singapore; [6]State Key Laboratory of Plant Physiology and Biochemistry, Department of Plant Sciences, College of Biological Sciences, China Agricultural University, Beijing 100193, China; [7]Department of Bioenergy Science and Technology, Chonnam National University, Buk-Gu, Gwangju 500-757, South Korea; [8]State Key Laboratory of Plant Genomics and National Plant Gene Research Center, Institute of Genetics and Developmental Biology, Chinese Academy of Sciences, Beijing 100101, China

The puzzle piece-shaped *Arabidopsis* leaf pavement cells (PCs) with interdigitated lobes and indents is a good model system to investigate the mechanisms that coordinate cell polarity and shape formation within a tissue. Auxin has been shown to coordinate the interdigitation by activating ROP GTPase-dependent signaling pathways. To identify additional components or mechanisms, we screened for mutants with abnormal PC morphogenesis and found that cytokinin signaling regulates the PC interdigitation pattern. Reduction in cytokinin accumulation and defects in cytokinin signaling (such as in *ARR7*-over-expressing lines, the *ahk3cre1* cytokinin receptor mutant, and the *ahp12345* cytokinin signaling mutant) enhanced PC interdigitation, whereas over-production of cytokinin and over-activation of cytokinin signaling in an *ARR20* over-expression line delayed or abolished PC interdigitation throughout the cotyledon. Genetic and biochemical analyses suggest that cytokinin signaling acts upstream of ROPs to suppress the formation of interdigitated pattern. Our results provide novel mechanistic understanding of the pathways controlling PC shape and uncover a new role for cytokinin signaling in cell morphogenesis.

Keywords**:** *Arabidopsis*; pavement cells; cytokinin; cell morphogenesis

Cell Research (2013) **23**:290-299. doi:10.1038/cr.2012.146; published online 23 October 2012

Introduction

Cytokinin is a crucial phytohormone that modulates many important developmental processes and responses to the environment including embryogenesis, seed development, organogenesis, vascular patterning, senescence, and stress tolerance [1-8]. At the cellular level, cytokinin is known to promote cell division, stem-cell specification, and chloroplast biogenesis [9-12]. The major cytokinin biosynthetic pathway is mediated by adenosine phosphate-isopentenyltransferase (IPT), which catalyzes the first and rate-limiting step [13, 14]. The structural diversity of natural cytokinins and modifications of the adenine moiety confer specificity of the cytokinin receptor interaction [14]. Cytokinin homeostasis is achieved through regulated conjugation or irreversible degradation [15], and cytokinin oxidase/dehydrogenase (CKX) catalyzes the irreversible degradation by cleavage of the side chain [14]. In *Arabidopsis*, three *Arabidopsis thaliana* histidine kinases serve as cytokinin receptors: AHK2, AHK3, and AHK4/CRE1/WOL [16-18]. The receptors

Correspondence: Zhenbiao Yang
E-mail: yang@ucr.edu
Received 16 May 2012; revised 24 July 2012; accepted 7 September 2012; published online 23 October 2012

are activated by autophosphorylation at a conserved histidine residue, and the phosphoryl group is transferred to *Arabidopsis* histidine phosphotransfer proteins (AHPs) [19]. AHPs (AHP1-AHP5) and nuclear response regulators serve as cytokinin signaling transcriptional regulators [3]. Based on domain structures and amino acid sequence similarities, the 22 *Arabidopsis* response regulators (ARRs) can be divided into two classes, type-A ARRs (ARR3-ARR9, ARR15-ARR17, ARR22) and type-B ARRs (ARR1, ARR2, ARR10-ARR14, ARR18-ARR21) [18, 20]. In general, type-B ARRs positively regulate the expression of cytokinin-induced genes, whereas type-A ARRs negatively regulate the gene expression [21-24].

Arabidopsis leaf pavement cells (PCs) form an interdigitated pattern with complementary lobes and indentations through the development of interdigitated multipolarity and subsequent local expansion at each polar site [25]. Thus, the generation of interdigitated lobes and indentations in the two-dimensional plane of the leaf epidermis provides a nice model system to investigate the planar coordination of cell polarity and morphogenesis among cells within a tissue [25-31]. Our recent studies suggest that auxin locally coordinates lobe formation with indentation by activating two counteracting Rho GTPase-based signaling pathways: the lobe-promoting ROP2 pathway localized to the lobe-forming region, and the lobe-restricting (indentation-promoting) ROP6 pathway localized to the indenting region of the plasma membrane (PM) [28-30]. The ROP2 pathway induces the formation of cortical F-actin, inhibiting the internalization of PIN1 and leading to its polarized enrichment at the lobing region [28, 30, 32]. The ROP2 and ROP6 pathways mutually inhibit each other, maintaining the separation of ROP2 and ROP6 function and coordinating PM lobe and indentation formation within the PC [28-30]. The interdigitation of lobes and indentations is also coordinated between neighboring PCs [30]. Through stimulation of the putative cell surface auxin receptor ABP1, PIN1-exported extracellular auxin is proposed to activate not only the ROP2 pathway in the lobing regions, but also the ROP6 pathway in the complementary indenting regions of neighboring cells [28-30]. Thus, auxin acts as a self-organizing signal to locally coordinate the establishment of multi-polarity for the generation of the interdigitated cell pattern in the leaf epidermis [33]. However, it is unknown whether other signaling pathways also regulate the PC interdigitation and cell morphogenesis.

In this report, we demonstrate that AHK3/CRE1- and ARR-dependent cytokinin signaling modulates the PC interdigitation in *Arabidopsis*. Our findings reveal a new mechanism for the regulation of cell polarity and morphogenesis as well as a novel function for cytokinin in the modulation of these fundamental cellular processes.

Results

Identification of cytokinin-signaling components regulating the interdigitated cell pattern in PCs

To investigate the mechanisms underlying the interdigitated pattern of PC expansion, we screened for T-DNA insertion mutations altering the interdigitation pattern in cotyledon PCs. We previously found that bathing germinating seedlings in a liquid medium containing 5-20 nM synthetic auxin Naphthalene-1-acetic acid (NAA) induced rapid interdigitation of all PCs in cotyledons/leaves [30]. In addition, we observed the downward curling of cotyledons from one-week-old seedlings after incubation with liquid medium containing auxin (Figure 1A; Supplementary information, Figure S1A and S1B). Thus, the progressive activation of PC interdigitation, which is accompanied by extensive cell expansion, may be important to maintain the flat cotyledon surface. We reasoned that mutations that cause insensitivity to the auxin induction of cotyledon curling might identify mutations affecting the coordination of PC interdigitation. Consistent with this notion, we found that the auxin receptor *tir1 afb1 afb2 afb3* quadruple mutant and previously studied PC-defective mutants *abp1-5* and *rop2-1 rop4-1* [30] showed a relatively flat cotyledon surface phenotype after NAA treatment (Supplementary information, Figure S2). Therefore, we screened an activation-tagged T-DNA insertional mutant library for such mutants and then analyzed their PC interdigitation. We screened 240 000 seedlings that covered 62 000 individual lines from 208 activation-tagging pools. This screen, along with a screen for abnormal leaf shape mutants, identified two groups of mutants with altered PC interdigitation patterning: group A with PCs having premature and enhanced interdigitation and group B with PCs showing reduced interdigitation (Figure 1B). From each group of more than 100 candidates, we cloned 11 genes belonging to group A and 12 genes in group B.

TAIL-PCR analysis revealed that each group contained an *ARR* gene that participates in cytokinin signaling [9, 22, 34]. Group A includes ARR7 (Supplementary information, Figure S2), a type-A ARR, that negatively regulates cytokinin signaling through repression of type-B ARRs. Group B includes ARR20, a type-B ARR, that positively regulates cytokinin signaling. The T-DNAs were inserted 2 301 bp and 1 553 bp upstream of the *ARR7* and *ARR20* start codons, respectively, suggesting that both genes were activation-tagged (Figure 1C). A semi-quantitative RT-PCR analysis confirmed that

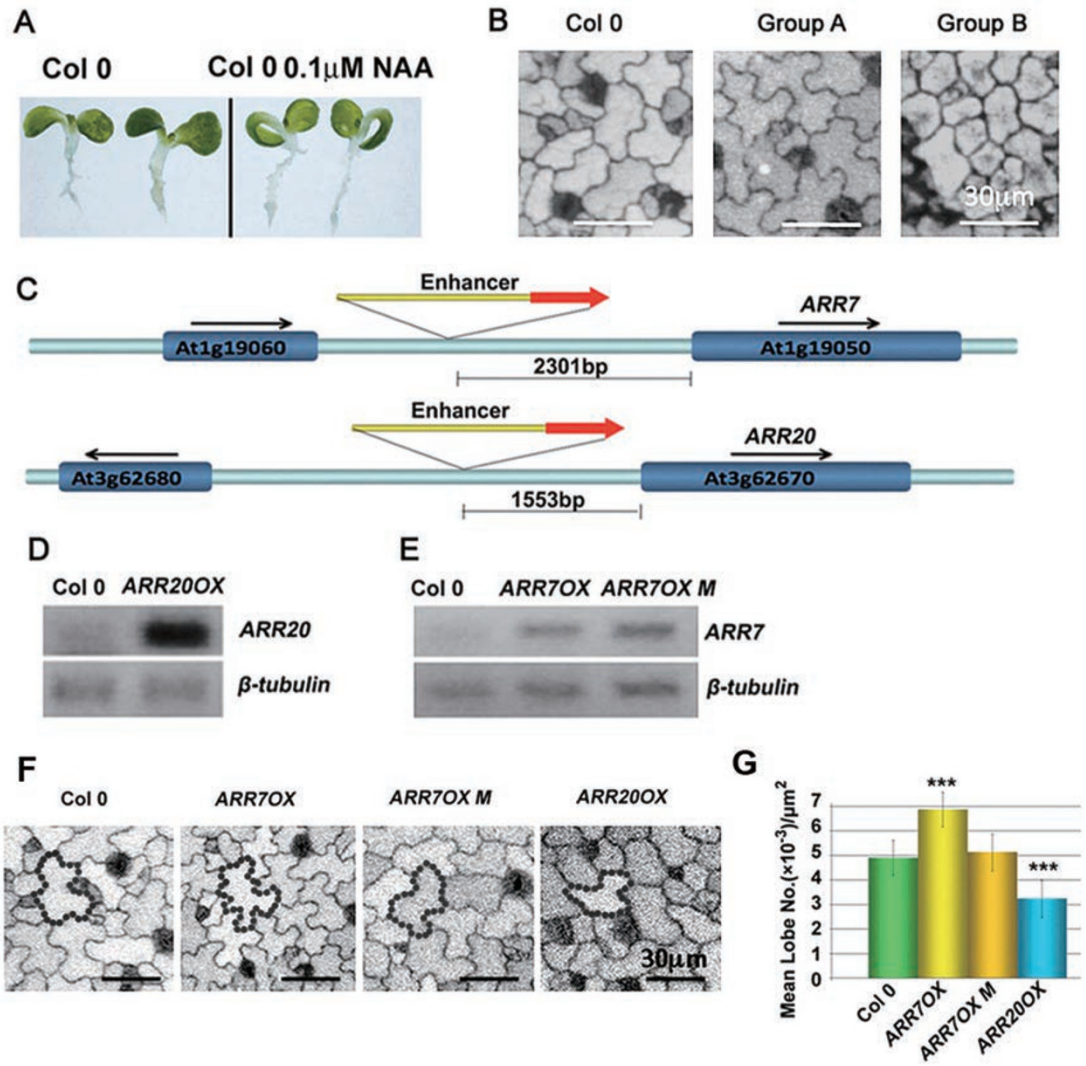

Figure 1 Genetic screen leading to the isolation of cytokinin signaling mutants that are altered in the PC interdigitation pattern. **(A)** Treatment with 0.1 μM NAA in liquid medium induced downward curling of cotyledons in 1-week-old Col-0 seedlings. **(B)** Representative images of 2-DAG (Days After Germination) cotyledons with altered PC interdigitation patterns in two groups of mutants. Group A mutants displayed more lobes, while group B mutants showed fewer lobes. Bars = 30 μm. **(C)** T-DNA insertion sites in *ARR7* (At1g19050) and *ARR20* (At3g62670) genes. The 35S enhancer sequences were inserted 2 301 bp and 1 553 bp upstream of the start codons of *ARR7* and *ARR20*, respectively. **(D)** RT-PCR analysis of *ARR20* transcript levels in the *ARR20OX* T-DNA insertion line. **(E)** RT-PCR analysis of *ARR7OX* and *ARR7OX M* transcript levels in the *ARR70X* and *ARR7OX M* lines. *ARR7OX M (D85N)* contains a point mutation in the D85 phosphorylation site that abolishes the function of ARR7 [24]. **(F)** Representative images of PC morphology in 2-DAG cotyledons of the *ARR7OX*, *ARR7OX M* and *ARR20OX* lines in the absence of benzyladenine (BA). Bars = 30 μm. **(G)** Quantitative analysis of lobe number per area (mean ± SEM) in the lines described in **F**. Quantitative analysis of cotyledon PC shape in greater than 400 PCs. The quantification of PC interdigitation is according to a previously described method [30]. Asterisks indicate significant differences from the wild-type control ($P < 0.001$, *t* test).

ARR20 was strongly over-expressed in the activation-tagged line designated as *ARR20OX* (Figure 1D). Quantitative analysis of the lobing phenotype showed that the number of lobes was greatly reduced in cotyledon PCs of the *ARR20OX* line (Figure 1F and 1G). In the T-DNA insertion line from group A, a moderate increase in *ARR7* mRNA level was observed in the T-DNA insertion line. To determine whether the enhanced lobing phenotype was due to *ARR7* over-expression, we analyzed PC shapes in a previously described p*35S::ARR7* line designated as *ARR7OX* [24]. *ARR7OX* PCs exhibited a significantly increased number of lobes (Figure 1E-1G).

Over-expression of the *ARR7 (D85N)* mutant designated as *ARR7OX M*, which has a defective phospho-accepting site and is unable to transmit cytokinin signal [24], did not alter the PC interdigitation pattern (Figure 1F and 1G). Therefore, we hypothesize that cytokinin signaling might regulate PC interdigitation.

Regulation of cytokinin levels affects PC interdigitation

Cytokinin is a multi-functional hormone that modulates many growth and developmental processes in plants. To determine whether cytokinin directly regulates PC interdigitation patterns, we induced changes in cytokinin levels in cotyledons through the dexamethasone (DEX)-induced expression of adenylate isopentyltransferase 7 (*IPT7*) or cytokinin oxidase 3 (*CKX3*). IPT7 catalyzes the rate-limiting first step of cytokinin biosynthesis [14], while CKX3 catalyzes cytokinin degradation [14]. DEX induction of *IPT7* expression in cotyledons greatly reduced PC lobe formation (Figure 2A and 2B). Treatment of cotyledons with exogenous cytokinin (50 nM) also inhibited PC interdigitation (Figure 3C and 3D). On the contrary, DEX induction of *CKX3* expression in cotyledons significantly enhanced PC interdigitation (Figure 2C and 2D). These results, together with the effects of *ARR7* and *ARR20* over-expression, demonstrate that cytokinin inhibits PC interdigitation.

The CRE1 and AHK cytokinin receptors regulate cytokinin-mediated cell interdigitation

We next examined whether cytokinin regulates PC interdigitation through the known histidine kinase (AHK) cytokinin receptor family comprised of three functionally redundant/overlapping members, CRE1/AHK4, AHK2, and AHK3, which activate cytokinin signaling by phospho-relaying to downstream ARRs [16, 35]. Based on the "*Arabidopsis* eFP Browser" [36], *AHK2*, *AHK3*, and *AHK4* are all expressed in cotyledons, although *AHK4* expression is quite weak; and similar expression patterns in rosette leaves for these *AHKs* have been reported [37]. We analyzed available single and double mutants of *AHKs*, including *ahk2-2*, *ahk3-3*, *cre1-12*, *ahk2-2 ahk3-3*, *ahk2-2 cre1-12*, *ahk3-3 cre1-12*, *ahk3-7 cre1-2,* and *cki1* (Figure 3A and 3B). Among these mutants, the dou-

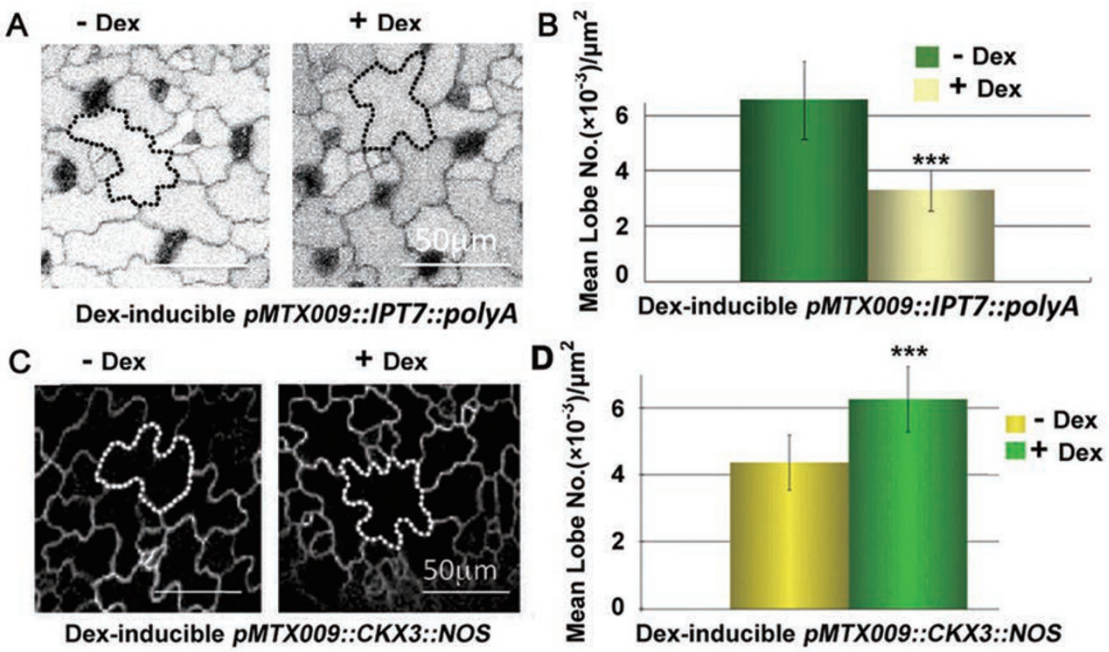

Figure 2 Cytokinin biosynthesis inhibits PC interdigitation. **(A)** Representative images of PC interdigitation in the 2 days presence or absence of DEX induced expression of *IPT7* (cytokinin biosynthetic enzyme) after 3-DAG *pMTX009::IPT7::polyA* seedlings. Bars = 50 μm. **(B)** Quantitative analysis of lobe number per area (mean ± SEM) after induction of *IPT7* expression by DEX treatment as described in **A**. Asterisks indicate significant differences from untreated seedlings ($P < 0.001$, *t* test). **(C)** Representative images of PC interdigitation in the 2 days presence or absence of DEX induced expression of *CKX3* (cytokinin degradation enzyme) after 2-DAG *pMTX009::CKX3::NOS* seedlings. Bars = 50 μm. **(D)** Quantitative analysis of lobe number per area (mean ± SEM) after induction of *CKX3* expression by DEX treatment as described in **C**. Asterisks indicate significant differences from untreated seedlings ($P < 0.001$, *t* test).

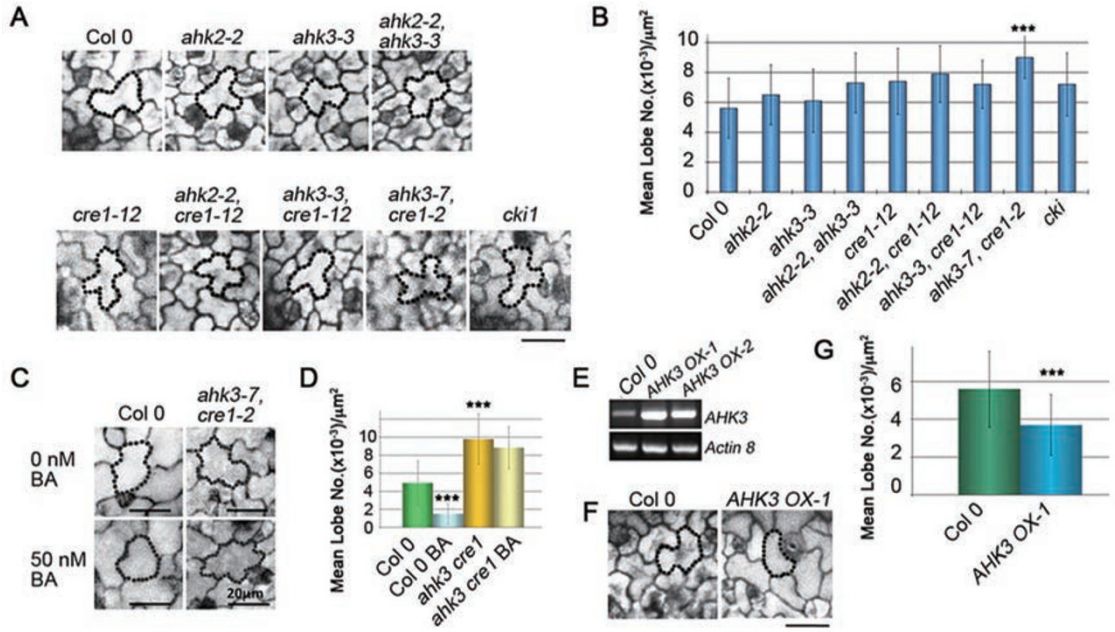

Figure 3 Cytokinin receptors regulate PC interdigitation. **(A)** Representative PC images of 2-DAG cotyledon PC shapes in Col 0 and different cytokinin receptor mutants. **(B)** Quantitative analysis of lobe number per area (mean ± SEM) in **A**. Asterisks indicate significant differences from Col 0 control ($P < 0.001$, *t* test). **(C)** Representative images of 2-DAG cotyledon PC shapes in wild type (WT) and the *ahk3 cre1* cytokinin receptor mutant both with and without BA treatment. Bars = 20 μm. **(D)** Quantitative analysis of lobe number per area (mean ± SEM) in the treatments described in **C**. Asterisks indicate a significant differences from untreated seedlings and WT (P <0.001, *t* test). The mean lobe number of *ahk3 cre1* PCs is $9.8\times10^{-3}/\mu m^2$, whereas WT PCs at the same stage have a mean lobe number of $4.7\times10^{-3}/\mu m^2$. **(E)** RT-PCR analysis of *AHK3* transcript level in two over-expression *AHK3* lines: *AHK3 OX-1* and *AHK3 OX-2*. **(F)** The representative PC images of 2-DAG *AHK3 OX-1* cotyledons compared with Col 0. Bars = 20 μm. **(G)** Quantitative analysis of lobe number per area (mean ± SEM) in **F**. Asterisks indicate significant differences from Col 0 seedlings ($P < 0.001$, *t* test).

ble loss-of-function mutant *ahk3-7 cre1-2* showed a clear change in the PC interdigitation pattern with precocious interdigitation in un-germinated cotyledons and greatly enhanced interdigitation in 2-DAG cotyledons (Figure 3A and 3B). The *ahk3-7 cre1-2* (*ahk3 cre1*) PCs were insensitive to exogenously applied synthetic cytokinin benzyladenine (BA), which severely inhibited PC interdigitation in wild-type cotyledons (Figure 3C and 3D). In addition, over-expression of *AHK3* (*AHK3 OX*) (Figure 3E) greatly decreased PC interdigitation in both cotyledons (Figure 3F and 3G) and true leaves (Supplementary information, Figure S3A and S3B). These results show that cytokinin acts through the functionally overlapping AHK3 and CRE1 to negatively regulate PC interdigitation and to prevent precocious interdigitation in the embryonic leaves during emobryogenesis.

Cytokinin suppresses PC interdigitation through a subset of ARR genes

A well-characterized mechanism downstream of the CRE1/AHK receptors involves phosphoryl relay from AHKs to ARRs through the histidine phospho-transfer proteins (AHPs) in *Arabidopsis*. Loss-of-function mutations in the five *AHP* genes (*ahp12345* quintuple mutant) abolishes the sensitivity to cytokinin in its regulation of various developmental processes [19]. Since we have shown that ARRs regulate PC interdigitation (Figure 1), we expect that AHPs would also affect this process. Indeed, the *ahp12345* mutant exhibited precocious and enhanced PC interdigitation in cotyledons, indicating that PC interdigitation is also regulated by the AHP-dependent mechanism (Figure 4A and 4B).

Both type-A and type-B ARRs are encoded by a gene family, and evidence suggests that certain subsets of ARRs have evolved to regulate a specific cytokinin-mediated process [23]. Because type-B, positive regulators of cytokinin signaling also controls the transcription of the type-A ARRs [23], we observed PC interdigitation in various type-A *ARR* over-expression lines. Among various type-A ARRs that negatively regulate cytokinin signaling [34], only over-expression of *ARR7* or its paralog *ARR15* enhanced PC interdigitation (Figure 4A

and 4B), suggesting that ARR7/ARR15 have diversified to regulate PC interdigitation patterns. These two ARRs are closely related, and represent an ARR clade that has evolved with a specific role for the regulation of PC interdigitation. In support of this, we found that the type-A *arr345689* hextuple mutant did not show obvious PC interdigitation defects, although it was reported to have other developmental defects, e.g. shorter roots, and to be more sensitive to cytokinin and less sensitive to red light than the wild type [22]. Neither *arr7* nor *arr15* single mutants showed obvious PC defects (Figure 4C and 4D; Supplementary information, Figure S4A), likely due to functional redundancy of these two ARRs, since both genes are expressed in cotyledons (*Arabidopsis* eFP Browser) [36].

Moreover, we analyzed various type-B *ARR* loss-of-function alleles in PC morphogenesis, and found that *arr20* shows increased PC interdigitation (Figure 4E and 4F; Supplementary information, Figure S4B), which is opposite to *ARR20OX*, with defects in PC interdigitation (Figure 1F and 1G). These data support the notion that ARR20 has evolved to specify the function in PC morphogenesis. In addition, we noticed that *arr11-1* shows a significant increase in PC interdigitation comparing to wild type (WT) (Supplementary information, Figure S4B), suggesting that ARR11 may have overlapping functions with ARR20. Nonetheless, we do not exclude the possibility that the other ARRs may also participate in the cytokinin signaling pathway that regulates PC interdigitation.

Cytokinin signaling acts upstream of ROPs in suppressing PC interdigitation

Since the ROP signaling pathways are required for PC interdigitation, we next asked whether cytokinin acts through or independent of these pathways. To assess the relationship between cytokinin and ROP signaling, we generated the *rop2*$^{-/-}$, *rop4*$^{+/-}$ and *ARR7OX* triple mutant (*rop2,4 ARR7OX*). PCs of the triple mutant line showed defects similar to those in the *rop2,4* mutant (Figure 5A and 5B). Furthermore, we found that ROP2 activity is decreased in *ARR20OX* (Figure 5C and 5D). Taken together these results suggest that cytokinin signaling acts upstream of ROPs to suppress the formation of the interdigitated pattern.

Discussion

The cellular basis for the phytohormonal control of developmental and morphogenetic processes has been linked to the regulation of cell growth, cell division, and cell fate specification. Our results expand the known

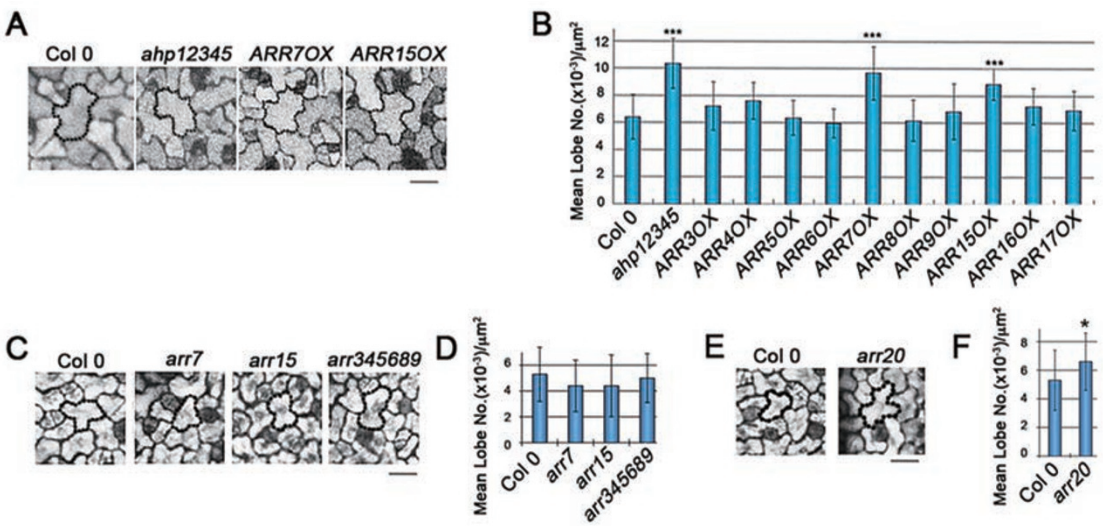

Figure 4 Components of the cytokinin signaling pathway regulate PC interdigitation. **(A)** Representative images of the PC morphology of 2-DAG cotyledons in Col 0, *ahp12345*, *ARR7OX*, and *ARR15OX*. Bar = 20 μm. **(B)** Quantitative analysis of lobe number per area (mean ± SEM) in cotyledon PCs of lines with an impaired regulation of cytokinin signaling, including the *ahp12345* pentuple loss-of-function mutant for the positive regulator AHPs, and transgenic lines over-expressing the indicated negative regulator type-A *ARRs*. Asterisks indicate a significant increase relative to wild-type PCs ($P < 0.001$, *t* test). **(C)** Representative images of the PC morphology of 2-DAG cotyledons in Col 0, *arr7*, *arr15* and *arr345689* loss-of-function mutants. Bar = 20 μm. **(D)** Quantitative analysis of lobe number per area (mean ± SEM) in **C**. **(E)** Representative images of the PC morphology of 2-DAG cotyledons in Col 0 and *arr20* loss-of-function mutants. Bar = 20 μm. **(F)** Quantitative analysis of lobe number per area (mean ± SEM) in **E**. Asterisks indicate a significant increase relative to wild-type PCs ($P < 0.05$, *t* test).

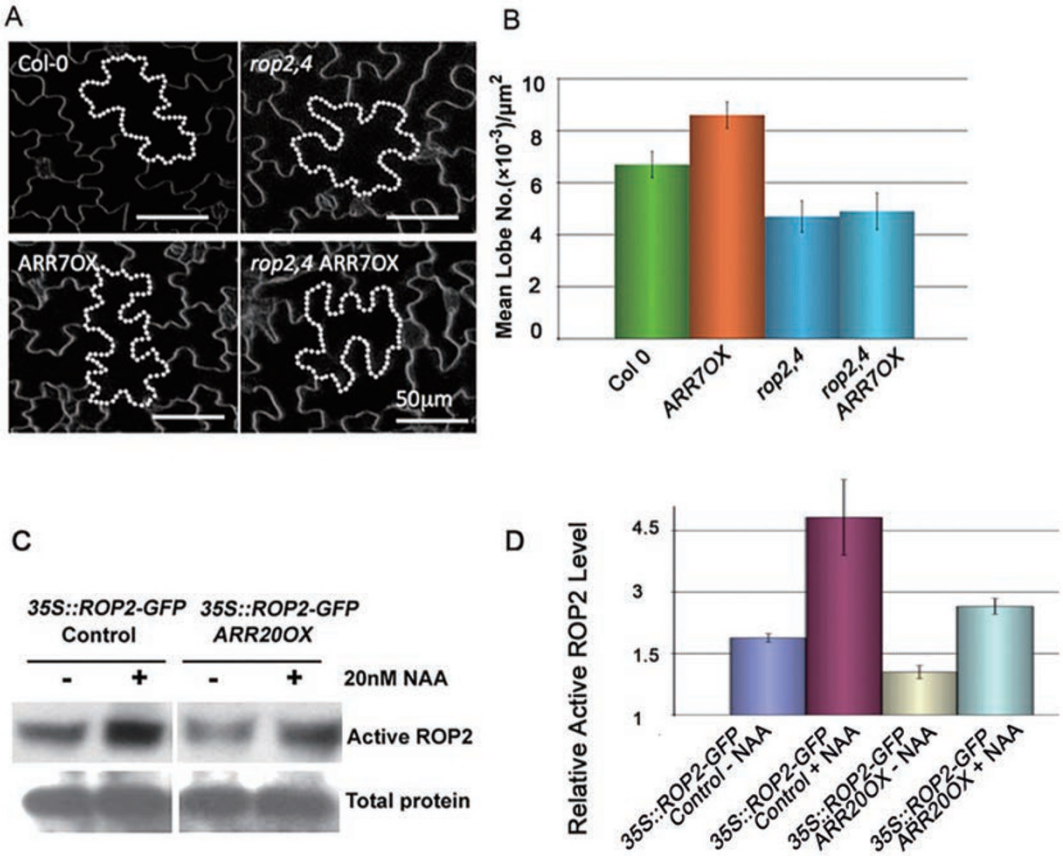

Figure 5 Cytokinin signaling acts upstream of ROPs to suppress the PC interdigitation. **(A)** Representative images of 4-DAG cotyledon PC shapes in WT, *ARR7OX*, *rop2,4*, and *rop2,4 ARR7OX*. Bars = 50 μm. **(B)** Quantitative analysis of lobe number per area (mean ± SEM) in WT, *ARR7OX*, *rop2,4*, and *rop2,4 ARR7OX*. **(C)** Auxin rescued the defect in ROP2 activation in *ARR20OX*. ROP2 activity was assayed using a pull-down assay as previously described (see Materials and Methods). *ARR20* over-expression reduced the endogenous ROP2 activity, but exogenously applied NAA (20 nM) greatly increased ROP2 activity to a level similar to or higher than that in untreated wild-type seedlings. **(D)** Quantitative analysis of relative ROP2 activity in *ARR20OX*.

roles of cytokinin signaling in plant development to include the regulation of cell morphogenesis. Our findings here, together with several recent findings on the new roles of auxin and cytokinin, suggest that the small molecule phytohormones play an important role in the spatial regulation of fundamental cellular processes such as cell polarity formation and cell morphogenesis. This adds a new dimension to cellular mechanisms for phytohormone action in plant growth and development. Auxin has recently been shown to regulate PC morphogenesis and polar distribution of PIN proteins by activating ROP GTPases [30, 32, 38]. Auxin has also been implicated in the regulation of the orientation of cell division by affecting microtubule organization [39]. Cytokinin is known to interact with auxin through the regulation of genes that are involved in the TIR1/AFB-based auxin signaling [9, 40]. However, recent studies suggest that cytokinin also modulates auxin function by directly regulating PIN degradation, consequently influencing PIN polar distribution and polar auxin transport [8, 41]. Our results, showing that cytokinin signaling regulates PC morphogenesis and ROP GTPase activity, further support a direct role for cytokinin signaling in the spatial regulation of fundamental cellular processes.

Our results suggest that cytokinin signaling provides a new mechanism for the regulation of PC morphogenesis, adding another developmental process regulated by auxin and cytokinin. We previously showed that auxin promotes PC interdigitation by activating ROP GTPases [30]. Interestingly, we found that cytokinin signaling suppresses PC interdigitation, suggesting that cytokinin and auxin have opposing roles in this process in a concentration-dependent manner (Supplementary information, Figure S5). Indeed our results showed that an increasing

concentration of NAA could rescue PC interdigitation defects induced by cytokinin (Supplementary information, Figure S5). Therefore, cytokinin regulation of the fundamental cellular process (cell morphogensis) appears to follow the common theme for the coordination of various developmental and morphogenetic processes in different tissues/organs involving a balancing act between cytokinin and auxin, although detailed mechanisms for the auxin-cytokinin balancing act may differ in different processes [1, 5, 6, 8-11, 42].

How does cytokinin antagonize the action of auxin in PC morphogenesis? Our data suggest that cytokinin acts upstream of ROP GTPases (Figure 5), and thus it is likely that cytokinin suppresses PC interdigitation by directly down-regulating ROP GTPase activity, as we have shown that ROP2 activity is inhibited by cytokinin signaling. However, our data do not exclude the possibility that cytokinin regulates ROP activity through the modulation of auxin levels, which are critical for PC interdigitation and ROP activation [30]. In addition, there are other possible mechanisms for cytokinin's action in suppressing PC interdigitation. Polar PIN1 distribution to the lobe tips in PCs has been shown to be required for PC interdigitation [30]. Cytokinin is known to affect PIN1 levels and PIN distribution in root morphogenesis [8, 41]. Thus a similar regulation of PIN1 in PCs might also participate in the control of PC interdigitation. Future research should be directed at exploring the mechanistic connection between cytokinin and auxin signaling in the regulation of PC morphogenesis.

Materials and Methods

NAA treatment and mutant screen

NAA (Sigma, St. Louis, MO) was dissolved in DMSO as a 0.5 M stock solution prior to dilution in liquid Murashige-Skoog (MS) media. Seeds were germinated in liquid MS media containing the indicated concentrations of NAA. Per 150 mm plate containing a sterilized filter paper at the bottom, approximately 1 000 seeds were added prior to addition of ½ MS media containing 100 nM NAA to cover the seeds. At 10 DAG (Days after germination), most of the seedlings would have expanded and curved cotyledons (Figure 1A). Seedlings with flat cotyledons were selected as the mutant candidates. Prior to transfer to soil, candidates were further grown in fresh auxin liquid medium for a few days to ensure the cotyledon did not curve after extended auxin treatment.

Materials and growth conditions

Arabidopsis plants were grown at 22 °C on ½ MS agar or in soil with 16 h-light /8 h-dark cycles. The majority of the mutant or transgenic lines used in this work were previously described, including *ARR7OX* (*35S::ARR7*) and *ARR7OX M* (*D85N*) [24], *ahk3 cre1* (*ahk3-7 cre1-2*) [2], *ahp12345* (*ahp1,2-2,3,4,5* quintuple mutant) [43], various type-A *ARR* over-expression lines (*ARR3OX*, *ARR4OX*, *ARR5OX*, *ARR6OX*, *ARR7OX*, *ARR8OX*, *ARR9OX*, *ARR15OX*, *ARR16OX*, *ARR17OX*) [34], and *cre1-12*, *ahk2-2*, *ahk3-3*, *ahk2-2 ahk3-3*, *ahk2-2 cre1-12*, *ahk3-3 cre1-12* [37]. *ARR20OX* (At3g62670) was obtained from the Ohio State University Arabidopsis Biological Resource Center. The type-A and type-B *ARR* loss-of-function Salk lines were obtained from ABRC or NASC: *arr1* (CS6971), *arr1-3 arr12-1* (N6981), *arr1-3 arr10-5 arr12-1* [44], *arr2-1* (SALK_043107), *arr2-4* (CS6975), *arr3* (SALK_042068C), *arr4* (CS25266), *arr5* (CS25267), *arr6* (SALK_133123C and SALK_080024C), *arr3456* (CS25276), *arr345689* (CS25279), *arr7* (N858131), *arr8* (SALK_057940C), *arr8 arr9* (CS25275), *arr10-1* (CS6990, Ws background), *arr11-1* (N6370, Ws background), *arr12-1* (CS6978), *arr13* (SALK_042719C), *arr14* (SALK_630_D09), *arr15* (GK_123D02.01), *arr16* (N873779), *arr17* (N873297), and cki1 (CS6360). The primers' sequences for genotyping type A and type B ARRs can be found in Supplementary information, Table S1. The accession of *pMTX009::IPT7::polyA* and *pMTX009::CKX3::NOS* lines are *Ler* (Landsberg *erecta*).

Microscopic analysis of PC shape

Cell outlines of PCs were visualized using UV laser (at 351 nm or 364 nm, 50% laser power and emission at 400-600 nm) under a Leica SP2 confocal microscope [30], including Figures 1B, 1F, 2A, 3A, 3C, 3F, 4A, 4C, and 4E. Alternatively, cell outlines were visualized by staining the PM with 5 μg/ml FM4-64 or FM1-43 dye for half an hour, and imaged using confocal microscopy with TRITC or FITC channels, respectively (Figures 2C and 5A). Stack images (1.0- to 2.0-μm increments) were collected from at least 200 cells from 5 individual plants, as described previously [30]. Additional image analysis was conducted by using MetaMorph software [30]. Adobe Photoshop CS was used for text editing of all images. Lobe numbers were quantified by number/area. Results are shown as mean numbers with standard error bars. For *t* test, the significance (triple asterisks) was set at $P < 0.001$, and one asterisk was set at $P < 0.05$.

We analyzed cotyledon PC phenotypes at different stages of seedlings, from 1-DAG seedling to plants with true leaves; the data we present in figures are the most pronounced phenotypes during the developmental stages. However, in most of the cases, the 2-DAG seedlings show the best phenotype and it is easy to quantify lobe numbers before the secondary lobes start to occur. Based on treatment and purpose of experiment, different developmental stages of PC are required. For example, Figure 2A, in order to see the decreasing lobes after treatment, we had to choose the stage, which had already formed enough lobes, for DEX treatment to observe maximal changes induced by cytokinin overaccumulation. In Figure 2B, we had to choose a relatively early stage when there were not many lobes for each cell. This allowed the observation of the differences induced by cytokinin degradation. The different developmental stages of seedlings we presented in figures are mentioned in each figure legend.

Regarding different confocal methods, we had to use FM4-64 staining only when it is very difficult to observe by UV, for example, large seedlings or plants with true leaves, for which the UV scanning signal was weak and unclear. We have attempted to use the same method as much as possible, however, in order to present the readers the clearest image, we had to use FM staining in some cases. Generally speaking, the UV laser is suitable for very small seedlings. We use staining method for those samples that give dif-

ficulties for observation by UV laser.

RT-PCR

Total RNA from cotyledons was isolated using RNeasy Plant Mini Kit (Qiagen). Reverse transcription was performed using SuperScript II (Invitrogen). Specific transcript levels were analyzed by RT-PCR relative to a *tubulin* loading control. Primer pairs used were tubulin_F: TTCCGTACCCTCAAGCTCGCTAAT, tubulin_R: ATCCTCTCGATGTCAATGGTGCGA. ARR7_F: AGAGTGGAACTAGGGCTTTGCAGT, ARR7_R: CTCCTTCTTTGAGACATTCTTGTATACGAGG. ARR20_F: CATCTCCAGAAGTACCGTCAAAG, ARR20_R: GGCTGCAAGAGTGACATCTG. AHK3 RT-F: GGAGGTGCGGTTTGATTTG, AHK3 RT-R: GGCTGGTTGTTGTCATTCTTTC. Actin 8F: CACATGCTATCCTCCGTCTC, Actin 8 R: CAATGCCTGGACCTGCTT.

Cytokinin treatment

Cytokinin treatments were conducted by germinating seeds in MS media containing cytokinin. A final concentration of 50 nM synthetic cytokinin BA was used.

Plasmid construction

The *IPT7* and *CKX3* genes were cloned from cDNA generated by RT-PCR. The cDNAs were first cloned into the *pENTR D-TOPO* vector (Invitrogen) and were sequenced to confirm error-free amplification. By employing Gateway methods the *polyA* terminator of the *35S* gene was added to *IPT7* and the *NOS* terminator was added to *CKX3*. Subsequently, the combined gene and terminator cassettes were inserted into the *Kpn*I and partially digested *Xho*I sites of *pPOPOFF2 (HYG)* [45] to generate *pMTX009::IPT7::polyA* and *pMTX009::CKX3::NOS* constructs.

For *AHK3 OX-1* and *AHK3 OX-2*, the *AHK3* (At1g27320) gene has been cloned into pFGC5941 by using the *Asc* I and *XBA* I cleavage sites. AHK3- *Asc* I: ggcgcgccATGAGTCTGTTCCATGTGCTAGG, AHK3-*XBA* I: tctagaTTATGATTCTGTATCTGAAGGCG.

DEX treatment

To induce *IPT7* or *CKX3* expression, a final concentration of 3 μM DEX was sprayed on *pMTX009::IPT7::polyA* or *pMTX009::CKX3::NOS* seedlings. The DEX spraying was repeated twice a day for two days, and the control seedlings had been sprayed by water. Treated seedlings and control were used for cotyledon PC shape analysis.

ROP2 activity assay

GFP-tagged active ROP2 was pulled down by use of MBP-RIC1 as described previously [30]. Protoplasts were isolated from leaves of 2- to 3-week-old *35S::GFP-ROP2 Arabidopsis* plants. Second or third pair rosette leaves were used to prepare protoplasts as described previously [46]. Protoplasts were counted by using a hemacytometer (Hausser scientific, Cat # 1483). Isolated protoplasts were treated with 20 nM NAA for 2 min and frozen by liquid nitrogen. Total protein was extracted from 10^5-10^6 treated protoplasts by extraction buffer (25 mM HEPEs pH 7.4; 10 mM $MgCl_2$; 10 mM KCl; 5 mM DTT; 5 mM Na_3VO_4; 5 mM NaF; 1 mM PMSF; 1% protease inhibitor from Sigma, St. Louis; 1% TritonX-100). A part of total proteins was used as control to determine the total amount of GFP-ROP2 (GDP-bound and GTP-bound). A saturated amount of MBP-RIC1-conjugated beads was added to the same amount of protoplast extracts from mutants with/without NAA treatment, which were then gently shaken at 4 °C for 3 h. Beads were washed in a washing buffer (25 mM HEPEs pH 7.4; 1 mM EDTA; 5 mM $MgCl_2$; 1 mM DTT; 0.5% TritonX-100) for three times at 4 °C (5 min each). Western blotting with anti-GFP antibody was used for analysis of the GTP-bound active form of GFP-ROP2 that was associated with the MBP-RIC1 beads (Santa Cruz Biotechnology, Santa Cruz, CA, USA).

Acknowledgments

We thank Dr Thomas Schmülling from Free University of Berlin, Germany for *ahk3-7 cre1-2* mutant. We thank Dr Tatsuo Kakimoto from Osaka University, Japan for *cre1-12, ahk2-2, ahk3-3, ahk2-2 ahk3-3, ahk2-2 cre1-12, ahk3-3 cre1-12* mutants. We are grateful to members of the Yang group for stimulating discussion during the course of this work. We thank Xinyan Zhang in Guo lab for sharing part of the SALK lines. This work was supported by grants from the US National Institute of General Medical Sciences (GM081451 and GM081451-03S2) to ZY. We thank National Science Foundation grant (IOS-1147250) to GVR and MX. HL and DL were partially supported by the Chinese Scholarship Council.

References

1 Aloni R, Aloni E, Langhans M, Ullrich CI. Role of cytokinin and auxin in shaping root architecture: regulating vascular differentiation, lateral root initiation, root apical dominance and root gravitropism. *Ann Bot* 2006; **97**:883-893.
2 Riefler M, Novak O, Strnad M, Schmulling T. *Arabidopsis* cytokinin receptor mutants reveal functions in shoot growth, leaf senescence, seed size, germination, root development, and cytokinin metabolism. *Plant Cell* 2006; **18**:40-54.
3 Muller B, Sheen J. *Arabidopsis* cytokinin signaling pathway. *Sci STKE* 2007; **2007**: cm5.
4 To JP, Kieber JJ. Cytokinin signaling: two-components and more. *Trends Plant Sci* 2008; **13**:85-92.
5 Bishopp A, Help H, El-Showk S, *et al.* A mutually inhibitory interaction between auxin and cytokinin specifies vascular pattern in roots. *Curr Biol* 2011; **21**:917-926.
6 Bishopp A, Lehesranta S, Vatén A, *et al.* Phloem-transported cytokinin regulates polar auxin transport and maintains vascular pattern in the root meristem. *Curr Biol* 2011; **21**:927-932.
7 Kushwah S, Jones AM, Laxmi A. Cytokinin-induced root growth involves actin filament reorganization. *Plant Signal Behav* 2011; **6**:1848-1850.
8 Marhavy P, Bielach A, Abas L, *et al.* Cytokinin modulates endocytic trafficking of PIN1 auxin efflux carrier to control plant organogenesis. *Dev Cell* 2011; **21**:796-804.
9 Muller B, Sheen J. Cytokinin and auxin interaction in root stem-cell specification during early embryogenesis. *Nature* 2008; **453**:1094-1097.
10 Moubayidin L, Di Mambro R, Sabatini S. Cytokinin-auxin crosstalk. *Trends Plant Sci* 2009; **14**:557-562.
11 Ruzicka K, Simásková M, Duclercq J, *et al.* Cytokinin regulates root meristem activity via modulation of the polar auxin transport. *Proc Natl Acad Sci USA* 2009; **106**:4284-4289.
12 Kobayashi K, Baba S, Obayashi T, *et al.* Regulation of root

greening by light and auxin/cytokinin signaling in *Arabidopsis*. *Plant Cell* 2012; **24**:1081-1095.
13 Kakimoto T. Identification of plant cytokinin biosynthetic enzymes as dimethylallyl diphosphate: ATP/ADP isopentenyltransferases. *Plant Cell Physiol* 2001; **42**:677-685.
14 Sakakibara H. Cytokinins: activity, biosynthesis, and translocation. *Annu Rev Plant Biol* 2006; **57**:431-449.
15 Werner T, Kollmer I, Bartrina I, Holst K, Schmulling T. New insights into the biology of cytokinin degradation. *Plant Biol (Stuttg)* 2006; **8**:371-381.
16 Inoue T, Higuchi M, Hashimoto Y, *et al*. Identification of CRE1 as a cytokinin receptor from *Arabidopsis*. *Nature* 2001; **409**:1060-1063.
17 Ueguchi C, Sato S, Kato T, Tabata S. The AHK4 gene involved in the cytokinin-signaling pathway as a direct receptor molecule in *Arabidopsis thaliana*. *Plant Cell Physiol* 2001; **42**:751-755.
18 Kakimoto T. Perception and signal transduction of cytokinins. *Annu Rev Plant Biol* 2003; **54**:605-627.
19 Hutchison CE, Li J, Argueso C, *et al.* The *Arabidopsis* histidine phosphotransfer proteins are redundant positive regulators of cytokinin signaling. *Plant Cell* 2006; **18**:3073-3087.
20 Aoyama T, Oka A. Cytokinin signal transduction in plant cells. *J Plant Res* 2003; **116**:221-231.
21 Kiba T, Yamada H, Sato S, *et al.* The type-A response regulator, ARR15, acts as a negative regulator in the cytokinin-mediated signal transduction in *Arabidopsis thaliana*. *Plant Cell Physiol* 2003; **44**:868-874.
22 To JP, Haberer G, Ferreira FJ, *et al.* Type-A *Arabidopsis* response regulators are partially redundant negative regulators of cytokinin signaling. *Plant Cell* 2004; **16**:658-671.
23 To JP, Deruère J, Maxwell BB, *et al*. Cytokinin regulates type-A *Arabidopsis* response regulator activity and protein stability via two-component phosphorelay. *Plant Cell* 2007; **19**:3901-3914.
24 Lee DJ, Kim S, Ha YM, Kim J. Phosphorylation of *Arabidopsis* response regulator 7 (ARR7) at the putative phosphoaccepting site is required for ARR7 to act as a negative regulator of cytokinin signaling. *Planta* 2008; **227**:577-587.
25 Yang Z. Cell polarity signaling in *Arabidopsis*. *Annu Rev Cell Dev Biol* 2008; **24**:551-575.
26 Fu Y, Li H, Yang Z. The ROP2 GTPase controls the formation of cortical fine F-actin and the early phase of directional cell expansion during *Arabidopsis* organogenesis. *Plant Cell* 2002; **14**:777-794.
27 Li S, Blanchoin L, Yang Z, Lord EM. The putative *Arabidopsis* arp2/3 complex controls leaf cell morphogenesis. *Plant Physiol* 2003; **132**:2034-2044.
28 Fu Y, Gu Y, Zheng Z, Wasteneys G, Yang Z. *Arabidopsis* interdigitating cell growth requires two antagonistic pathways with opposing action on cell morphogenesis. *Cell* 2005; **120**:687-700.
29 Fu Y, Xu T, Zhu L, Wen M, Yang Z. A ROP GTPase signaling pathway controls cortical microtubule ordering and cell expansion in *Arabidopsis*. *Curr Biol* 2009; **19**:1827-1832.
30 Xu T, Wen M, Nagawa S, *et al.* Cell surface- and rho GTPase-based auxin signaling controls cellular interdigitation in *Arabidopsis*. *Cell* 2010; **143**:99-110.
31 Li H, Lin D, Dhonukshe P, *et al*. Phosphorylation switch modulates the interdigitated pattern of PIN1 localization and cell expansion in *Arabidopsis* leaf epidermis. *Cell Res* 2011; **21**:970-978.
32 Nagawa S, Xu T, Lin D, *et al.* ROP GTPase-dependent actin microfilaments promote PIN1 polarization by localized inhibition of clathrin-dependent endocytosis. *PLoS Biol* 2012; **10**:e1001299.
33 Xu T, Nagawa S, Yang Z. Uniform auxin triggers the Rho GTPase-dependent formation of interdigitation patterns in pavement cells. *Small Gtpases* 2011; **2**:227-232.
34 Ren B, Liang Y, Deng Y, *et al.* Genome-wide comparative analysis of type-A *Arabidopsis* response regulator genes by overexpression studies reveals their diverse roles and regulatory mechanisms in cytokinin signaling. *Cell Res* 2009; **19**:1178-1190.
35 Sheen J. Phosphorelay and transcription control in cytokinin signal transduction. *Science* 2002; **296**:1650-1652.
36 Winter D, Vinegar B, Nahal H, Ammar R, Wilson GV, Provart NJ. An "Electronic Fluorescent Pictograph" browser for exploring and analyzing large-scale biological data sets. *PLoS One* 2007; **2**:e718.
37 Higuchi M, Pischke MS, Mähönen AP, *et al.* In planta functions of the *Arabidopsis* cytokinin receptor family. *Proc Natl Acad Sci USA* 2004; **101**:8821-8826.
38 Robert S, Kleine-Vehn J, Barbez E, *et al*. ABP1 mediates auxin inhibition of clathrin-dependent endocytosis in *Arabidopsis*. *Cell* 2010; **143**:111-121.
39 Dhonukshe P, Weits DA, Cruz-Ramirez A, *et al.* A PLETHORA-Auxin transcription module controls cell division plane rotation through MAP65 and CLASP. *Cell* 2012; **149**:383-396.
40 Dello Ioio R, Nakamura K, Moubayidin L, *et al*. A genetic framework for the control of cell division and differentiation in the root meristem. *Science* 2008; **322**:1380-1384.
41 Zhang W, To JP, Cheng CY, Eric Schaller G, Kieber JJ. Type-A response regulators are required for proper root apical meristem function through post-transcriptional regulation of PIN auxin efflux carriers. *Plant J* 2011; **68**:1-10.
42 Jones B, Gunnerås SA, Petersson SV, *et al.* Cytokinin regulation of auxin synthesis in *Arabidopsis* involves a homeostatic feedback loop regulated via auxin and cytokinin signal transduction. *Plant Cell* 2010; **22**:2956-2969.
43 Deng Y, Dong H, Mu J, *et al. Arabidopsis* histidine kinase CKI1 acts upstream of histidine phosphotransfer proteins to regulate female gametophyte development and vegetative growth. *Plant Cell* 2010; **22**:1232-1248.
44 Argyros RD, Mathews DE, Chiang YH, *et al*. Type B response regulators of *Arabidopsis* play key roles in cytokinin signaling and plant development. *Plant Cell* 2008; **20:**2102-2116.
45 Wielopolska A, Townley H, Moore I, Waterhouse P, Helliwell C. A high-throughput inducible RNAi vector for plants. *Plant Biotechnol J* 2005; **3**:583-590.
46 Sheen J. Signal transduction in maize and *Arabidopsis* mesophyll protoplasts. *Plant Physiol* 2001; **127**:1466-1475.

(**Supplementary information** is linked to the online version of the paper on the *Cell Research* website.)